



## **Deliverable 2.4: Report on squaring along (110) orientation assessment for manufacturability**

**Task 2.1: Developing new cost-effective and high-quality wafer manufacturing processes**

WP2: Ingot & Wafer

**Lead participant:** CEA  
**Delivery date:** 30/04/2024  
**Dissemination level:** Public  
**Type:** Report

## Document History

Date	Version	Prepared by	Organisation	Approved by	Notes
12/04/2024	V01	Mickael ALBARIC	CEA		
30/04/2024	V02	Samuel HARRISON	CEA		
10/05/2024	V02.1	Daiva Ulbikienė	PROTECH		Final editing
10/05/2024				Florian Buchholz	

## Acknowledgements

The work described in this publication has received funding from the European Union’s Horizon Europe energy research and innovation program under grant agreement N° 101084259.

## Disclaimer

This document reflects only the authors’ view and not those of the European Community. This work may rely on data from sources external to the members of the IBC4EU project Consortium. Members of the Consortium do not accept liability for loss or damage suffered by any third party as a result of errors or inaccuracies in such data. The information in this document is provided “as is” and no guarantee or warranty is given that the information is fit for any particular purpose. The user thereof uses the information at its sole risk and neither the European Community nor any member of the IBC4EU Consortium is liable for any use that may be made of the information.

© Members of the IBC4EU Consortium

### Project Partners



### Associated Partners



## Contents

<b>EXECUTIVE SUMMARY .....</b>	<b>6</b>
<b>1 INTRODUCTION .....</b>	<b>7</b>
<b>2 CONTEXT .....</b>	<b>7</b>
<b>3 45° SQUARING PRINCIPLE .....</b>	<b>9</b>
3.1 STEP 1: INGOT SECTION MARKING .....	10
3.2 STEP 2: SQUARING .....	10
3.3 STEP 3: INITIAL ANGLE MISORIENTATION MEASUREMENT .....	11
3.4 STEP 4: GRINDING .....	11
<b>4 KALYON INGOT.....</b>	<b>12</b>
4.1 45° INGOT SQUARING G1 SIZE .....	13
4.2 G1 45° ORIENTED BRICK IN KALYON INDUSTRIAL LINE.....	14
<b>5 NORSUN INGOT.....</b>	<b>15</b>
5.1 45° INGOT SQUARING M2 SIZE .....	16
5.2 STANDARD INGOT SQUARING M2 SIZE.....	17
5.3 BRICKS WAFERING .....	18
<b>6 CONCLUSION.....</b>	<b>18</b>
<b>7 GLOSSARY .....</b>	<b>19</b>
<b>8 REFERENCES .....</b>	<b>20</b>

## Figures

<b>Figure 1:</b> Brick orientation and fabrication of 45° rotated wafers, the (110) plane is set parallel to the wafer edges compared to a diagonal direction for standard wafers. ....	9
<b>Figure 2:</b> a. mechanical cleavage on „conventional“ cell; b. mechanical cleavage on „45° oriented“ cell.....	9
<b>Figure 3:</b> SEM pictures of the 45° rotated cut solar cells edges: a. global view of the edge b. zoom closer to the front surface. Both SEM show very smooth and uniform edge final cut morphologies.....	9
<b>Figure 4:</b> (110) plane marking on the ingot section .....	10
<b>Figure 5:</b> a. B.E.A squarer equipment (CEA) b. 45° oriented ingot squaring.....	11
<b>Figure 6:</b> Goniometer equipment (CEA) – (110) plane misorientation measurement .....	11
<b>Figure 7:</b> a. Arnold grinding equipment (CEA) b. 45° oriented brick grinding.....	12
<b>Figure 8:</b> G1 45° oriented brick, p-type boron doped Cz ingot provided by Kalyon .....	13
<b>Figure 9:</b> G1 45° oriented brick wafering - Kalyon .....	14
<b>Figure 10:</b> PERC cell efficiency: comparison between 45° oriented wafers and standard wafers.....	14
<b>Figure 11:</b> Example of mini-module made with two 45° oriented PERC half cell - Kalyon .....	15
<b>Figure 12:</b> M2 45° oriented brick, p-type gallium doped Cz ingot Norsun.....	16
<b>Figure 13:</b> a.M2 (100) plane marking ; b.M2 standard oriented brick, p-type gallium doped Cz ingot Norsun .....	17
<b>Figure 14:</b> Norsun M2 „standard“ wafers a. wafer pre-cleaning; b. wafer cleaning – Novatec equipments ..	18

## Tables

<b>Table 1:</b> Possible brick size fabrication at CEA. ....	12
<b>Table 2:</b> (110) plane misorientation measurements after squaring and grinding steps - Kalyon.....	13
<b>Table 3:</b> Mini-modules electrical measurements - Kalyon.....	15
<b>Table 4:</b> (110) plane misorientation measurements after squaring and grinding steps - Norsun.....	16
<b>Table 5:</b> (100) plane misorientation measurements after squaring and grinding steps - Norsun.....	17
<b>Table 6:</b> Wafer topology, comparison between M2 45° oriented wafer and standard wafers. Values averaged over 60 wafers- CEA.....	18

## Executive Summary

CEA carried out the development of the 45° squaring of ingots and initiated collaboration on the topic with the two industrial partners Kalyon (p type boron doped) and Norsun (p type gallium doped). According to wafers size constraints of the partners, two brick sizes has been successfully manufactured in such alternative configuration: a p-type Cz ingot doped with boron from Kalyon for G1 45° oriented brick squaring and a p-type Cz ingot doped with gallium from Norsun for M2 45° oriented brick squaring. For both configurations the (110) plane misorientations after grinding were lower than 0.3° which allows a mechanical cleavage between the metallization busbars of the future PV cells. Moreover, excellent results were obtained on the 45° wafers produced after integration in the different cell and module production lines (INES Labfab, and Kalyon Gigawatt Factory). In particular:

- No increase in breakage rate with this new wafer orientation was observed compared to standard Cz wafers usually integrated.
- Similar final efficiencies measured on the G1 45° oriented PERC cells processed by Kalyon when compared to standard production values observed in the factory.

## 1 Introduction

A clean half-cell separation process was elaborated at CEA. It is based on 45° rotated silicon brick and wafers fabrication, allowing the alignment of the preferential cleavage plan (110) with the solar cells bus bars. Consequently, the cell separation can be simply realized thanks to a short diamond tip scribe at the edge, followed by a mechanical bending stress to propagate a crack along the wafer, parallel to the cell's metal bus bars [1]. Therefore, no laser-assisted technique is needed, and the resulting edge appears as smooth as what can be obtained with the use of recent thermo-mechanical cleavage solutions proposed by the industry (TLS by 3D-Micromac or LDC by INNOLAS). Such superior edge morphology obtained thus with the 45° rotated wafers developed is thus particularly well adapted for the further application of efficient cut-edge (re)passivation solutions [2-3]. However, manufacturability and scaling-up of such cut and passivation solutions must be now evaluated in real production environment conditions, and joint evaluation results achieved by CEA, NORSUN and KALYON for this technology will be reported in this report.

## 2 Context

Half-cells or shingle module architectures have widely and quickly spread on the PV market to both ensure continuous increase of solar panel power (reduced resistive losses and increase of the usable area of the module) and new demands for adaptive PV modules (BIPV, VIPV, etc), while implying minimum technology alteration [4]. However, the electrical gain obtained at module level using half-cell or shingle configuration may be lessened by absolute cell efficiency loss resulting from half-cell cutting process or sub-cells in the case of shingle module architecture. Two main approaches are currently considered at industrial scale for half-cell cutting process: i) conventional laser scribe and break and ii) thermo-mechanical cleavage (TMC), where a controlled thermal gradient is used to propagate the cleavage crack initiated by laser shallow scribing on the edge of the wafer. The cutting step process generally induces edge defectivity which is especially impacting for low temperature cell architectures such as silicon heterojunction (SHJ) solar cells. Today, for any of the considered optimized cutting processes, the absolute cell efficiency loss is in the range of  $\sim 0.2$  to  $0.3\%_{Abs}$  for high efficiency SHJ when going from full to half-cell configuration [5-6] and can reach up to close to  $\sim 1\%_{Abs}$  loss in case of shingle configuration. Furthermore, with laser scribe and cleave approach, the local melting of the silicon cut-surface-induced surface morphology that usually totally avoids any application of edge repassivation process that may be applied to recover for the initial cut-cell efficiency losses. During the past years, CEA studied an alternative approach for solar heterojunction cell separation, based on the fabrication of the so-called  $45^\circ$  rotated wafers. For such wafers, the (110) privileged crystallographic planes are naturally aligned with the cell edges (Figure 1). Indeed, a standard silicon brick is generally shaped along (010) lateral planes and consequently the (110) preferential cleavage plane is located on the resulting wafer's diagonals. In our case, thanks to a simple  $45^\circ (\pm 0.1^\circ)$  rotation of the ingot during the squaring step applied to form the final brick, we modify the orientation of such cleavage plane and generate new wafer scheme with final (110) oriented lateral planes. Hence, we allow alignment of the preferential mechanical cleavage plane of the corresponding  $45^\circ$  oriented wafers parallel to the wafer edges (Figure 2), and most importantly, parallel to the metal pattern busbars where future cut is needed. This new wafer orientation allows the end user to get fully rid of laser assisted cleavage technologies, as simple mechanical edge scribing followed by mechanical cleavage is now possible, leading to final high edge morphology quality.

No modification of process is needed for the generation of  $45^\circ$  rotated wafers. Standard squaring and wafering process steps can then be applied to such ingots, with in particular the use of usual diamond wire-sawing equipment to generate the wafers. The resulting  $45^\circ$  rotated  $160 \mu\text{m}$  thick M2 (156.75 mm large) wafers were then successfully integrated on the industrial CEA-INES pilot line for the fabrication of SHJ solar cells [7-8]. No adaptation or modification of any fabrication step was necessary, and equivalent efficiencies and breakage rate observed for the newly  $45^\circ$  wafers when compared to the usual Cz references.

In the frame of IBC4EU project CEA supported NORSUN and KALYON to test and adapt this  $45^\circ$  rotated process to their own squaring and wafering systems with larger-compliant bricks. The objective being to validate that this approach can be fully compliant with full production environment and larger ingot/wafer sizes.





### 3 45° squaring principle

In this paragraph, the different fabrication steps of the 45° squaring are presented. It is good to note that the methodology presented here is in line with the equipment available at CEA: it is a "semi-manual" R&D mode compared to what is done today in the industry.

#### 3.1 Step 1: Ingot section marking

The objective of step1 is to mark the position of the (110) plane on the section of the ingot (Figure 4). To do this, it is necessary to locate the position of the 4 nodes on the surface of the ingot which are characteristics of a (100) Cz growth. The (110) plane are situated along "node1–node3" or "node2- node4" lines or parallels to these lines (figure 4). At this step, the mark made, representing the side of the brick, takes into account a margin of ~8 mm compared to the final size of the brick.

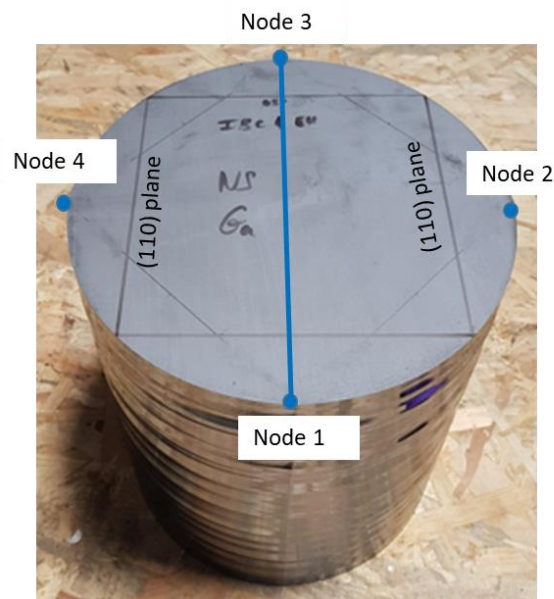
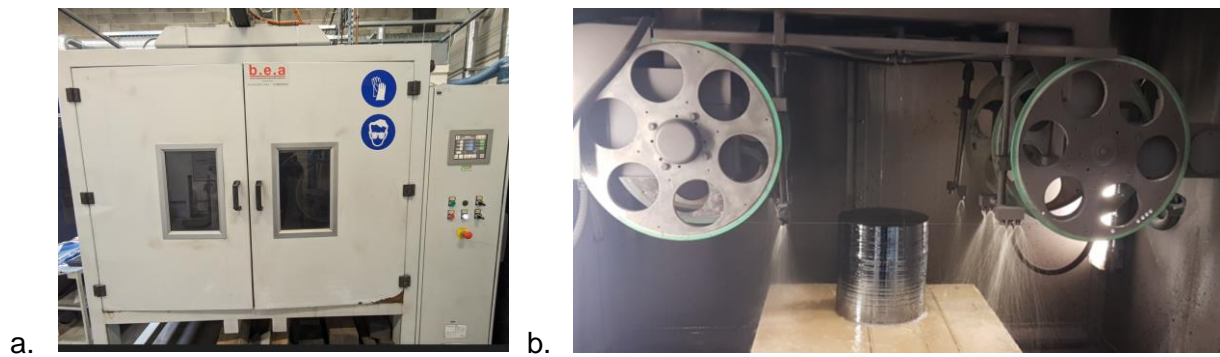


Figure 4: (110) plane marking on the ingot section

#### 3.2 Step 2: squaring

The squaring of the brick is performed with a "B.E.A" squarer using 0.6 mm diameter diamond wire (Figure 5). It is possible to cut two sides of the brick per cutting run, two cutting runs are thus necessary to square the brick.



**Figure 5:** a. B.E.A squarer equipment (CEA) b. 45° oriented ingot squaring

### 3.3 Step 3: initial angle misorientation measurement

Initial angle misorientation with the plane (110) are measured with a goniometer (Figure 6). From this measurement, the correction to be applied at the grinding step is computed.



**Figure 6:** Goniometer equipment (CEA) – (110) plane misorientation measurement

### 3.4 Step 4: Grinding

The grinding of the brick is performed with an “Arnold” grinding equipment (Figure 7). A wedging of the brick is carried out (up to 4mm) to take into account the correction to be applied (determined in the previous step). With each pass it is possible to remove up to 300  $\mu\text{m}$  of silicon. Once the final size of the brick is reached, two “finishing” passes at 20  $\mu\text{m}$  and 10  $\mu\text{m}$  are carried out on each face of the brick.

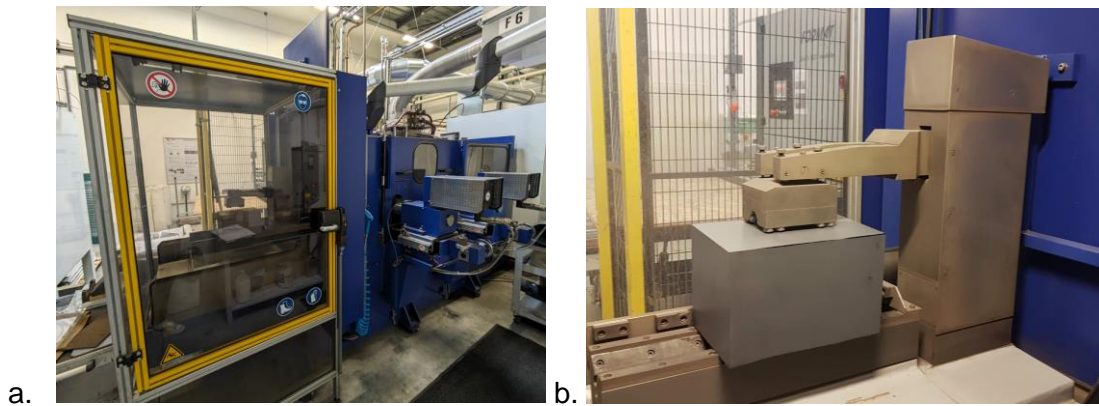


**Figure 7:** a. Arnold grinding equipment (CEA) b. 45° oriented brick grinding

According to the equipment available at CEA it is possible to square 45° oriented bricks until M6 size. The following table summarizes the different wafer formats that can be processed.

**Table 1:** Possible brick size fabrication at CEA.

Brick size	Lateral side (mm)	Chamfer (mm)
M2	156.75 x 156.75 ± 0.25mm Diameter: 210mm ± 0.25mm	11.68 ± 0.25mm
G1	158.75 x 158.75 ± 0.25 mm Diameter: 223mm ± 0.25mm	1.5 ± 0.25mm
M6	166 x 166 ± 0.25mm Diameter: 223mm ± 0.25mm	11.75 ± 0.25mm

After the grinding step, goniometer measurements are performed on the 4 sides of the brick to control the final angle misorientation with the (110) plane. The objective is to achieve a final misorientation of less than 0.3°.

## 4 Kalyon Ingot

Kalyon sent to CEA a 50 cm piece of p-type Cz ingot doped with boron for 45° oriented brick squaring. CEA prepared a G1 45° oriented brick and sent it back to Kalyon for wafering, cell processing and mini modules manufacturing. This CEA-Kalyon collaboration allowed thus to evaluate the potential of the 45° oriented wafers in a full industrial environment for most of the production chain.

### 4.1 45° ingot squaring G1 size

The G1 45° oriented brick squaring (figure 8) followed the principle presented in chapter 3. After the squaring step the initial misorientation to be corrected was in the range of +1.19° to 1.46° (Table 2). After grinding the final (110) angle misorientation finally obtained was in the 0.14° to 0.27° range which corresponds to a deviation of the cleavage plane along the cell side of 387µm to 730µm.

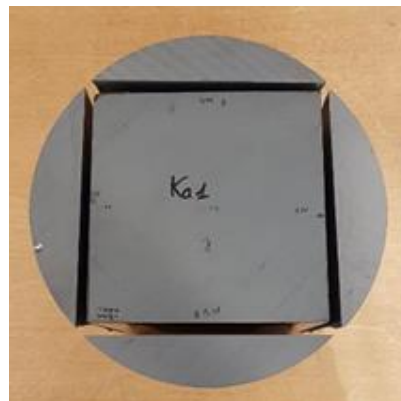


**Figure 8:** G1 45° oriented brick, p-type boron doped Cz ingot provided by Kalyon

**Table 2:** (110) plane misorientation measurements after squaring and grinding steps - Kalyon

45° squaring Kalyon	After squaring		After grinding	
	(110) Misorientation (°)	(110) Misorientation (°)	(110) Misorientation (°)	Cleavage deviation along the side of the cell (µm)
45° Ka1 brick face A	1.19	0.16	0.16	443
45° Ka1 brick face B	1.36	0.25	0.25	678
45° Ka1 brick face C	1.33	0.27	0.27	730
45° Ka1 brick face D	1.46	0.14	0.14	387

## 4.2 G1 45° oriented brick in Kalyon industrial line

The G1 45° oriented brick was sent to Kalyon for wafering, PERC cell processing and PV mini-module manufacturing in their production line. Excellent results were achieved on the 45° wafers produced:

- the G1 45° oriented brick was cut into 175  $\mu\text{m}$  thick wafers. No increase in breakage rate with new wafer orientation was observed compared to standard wafers (Figure 9),
- the efficiency of PERC cells generated is similar to standard production values observed in the factory (Figure 10). Two groups of wafers were used: 45° oriented (45DR) and standard (STD) for reference (~200 wafers each),
- mini-modules each composed of two half cells were manufactured at Kalyon for mechanical and electrical testing. Here again no increase in breakage rate was observed compared to mini module manufacturing with standard wafers (Figure 11 & Table 3).



Figure 9: G1 45° oriented brick wafering - Kalyon

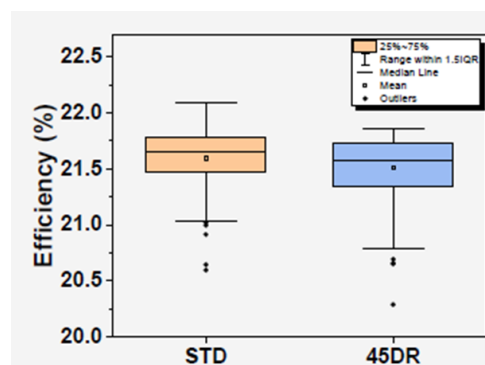


Figure 10: PERC cell efficiency: comparison between 45° oriented wafers and standard wafers



**Figure 11:** Example of mini-module made with two 45° oriented PERC half cell - Kalyon

**Table 3:** Mini-modules electrical measurements - Kalyon

Mini-modules	Parameters					
	Pmax(V)	Voc (V)	Isc (A)	Vpmax (V)	Ipmax (A)	FF (%)
45°-1	4.73	1.36	4.83	1.05	4.49	72.07
Standard-1	4.80	1.36	4.84	1.06	4.51	72.89
Standard-2	4.72	1.36	4.84	1.05	4.49	71.84
45°-3	4.75	1.36	4.80	1.06	4.49	72.69
Standard-3	4.71	1.35	4.81	1.06	4.45	72.23
Uncertainty	Pmax(V)	Voc (V)	Isc (A)	Vpmax (V)	Ipmax (A)	FF (%)
	%	%	%	%	%	%
	1.8	0.9	1.0	1.4	1.1	2.0

## 5 NORSUN Ingot

Norsun sent CEA a 50 cm piece of p-type Cz ingot doped with gallium for 45° oriented brick squaring. CEA prepared one M2 45° oriented brick and one M2 standard brick. The two bricks have been wafered by CEA and ~200 wafers were sent to ISFH for Polo-IBC cell integration.

### 5.1 45° ingot squaring M2 size

The M2 45° oriented brick squaring (figure 12) followed the principle presented in chapter 3. After the squaring step the initial misorientation to be corrected was in the  $-1.21^\circ$  to  $-1.35^\circ$  range (Table 4). After grinding the final (110) angle misorientation was in the  $-0.02^\circ$  to  $-0.13^\circ$  range which corresponds to a deviation of the cleavage plane along the cell side of  $55\mu\text{m}$  to  $355\mu\text{m}$ .

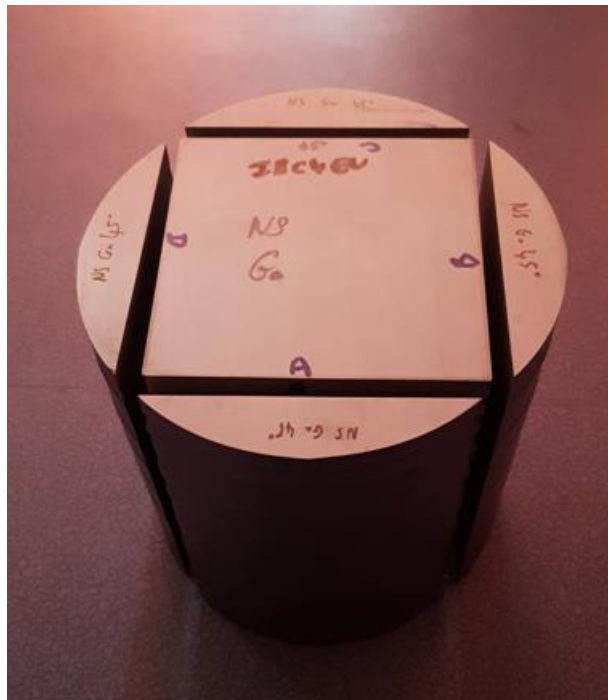


Figure 12: M2 45° oriented brick, p-type gallium doped Cz ingot Norsun

Table 4: (110) plane misorientation measurements after squaring and grinding steps - Norsun

45° squaring Norsun	After squaring	After grinding	
	(110) Misorientation (°)	(110) Misorientation (°)	Cleavage deviation along the side of the cell ( $\mu\text{m}$ )
45° NS1 brick face A	-1.32	-0.13	355



45° NS1 brick face B	-1.21	-0.12	314
45° NS1 brick face C	-1.30	-0.04	96
45° NS1 brick face D	-1.35	-0.02	55

### 5.2 Standard ingot squaring M2 size

To perform the (100) standard squaring it is necessary to locate the position of the 4 nodes on the surface of the ingot which are characteristics of a (100) Cz growth. The (100) plane are situated along "node1–node2" or "node2- node3" lines or parallels to these lines (figure 10.a). After the squaring and the grinding steps (figure 10.b) the (100) plane misorientations are in the range of -1.08° to -1.28° (Table 5). Here no angle correction was applied because the initial (100) plane misorientation achieved is in accordance with what is usually observed in industry.

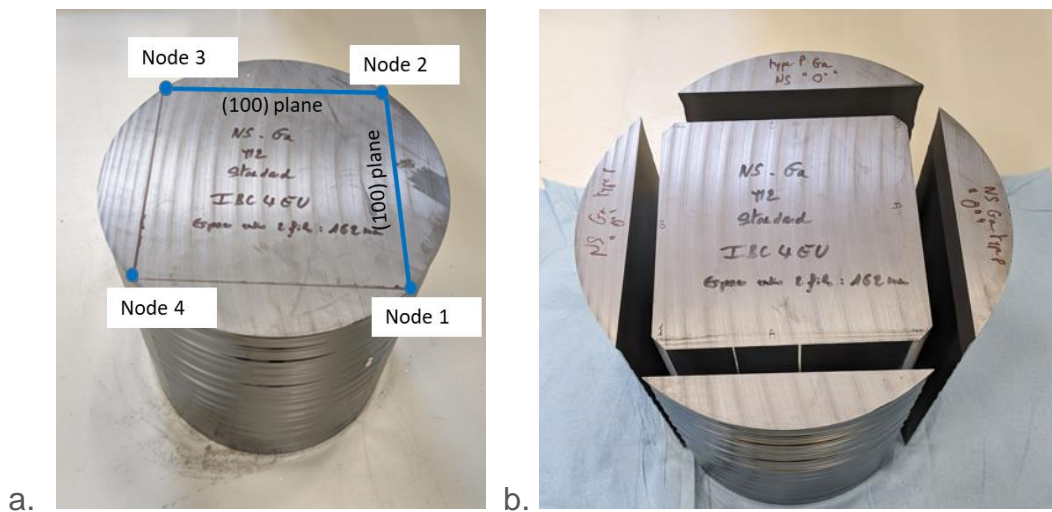


Figure 13: a.M2 (100) plane marking ; b.M2 standard oriented brick, p-type gallium doped Cz ingot Norsun

Table 5: (100) plane misorientation measurements after squaring and grinding steps - Norsun

Standard squaring Norsun	After squaring and grinding
	(100) Misorientation (°)
NS2 brick face A	-1.08
NS2 brick face B	-1.28
NS2 brick face C	-1.28
NS2 brick face D	-1.24

### 5.3 Bricks wafering

The two bricks were cut at CEA with the Meyer Burger DW288 sawing machine. For both bricks the diameter of the diamond wire used was 60 $\mu$ m and the target thickness of the wafers was 160  $\mu$ m.

During the wafering step no problem was observed. No increase in breakage rate with the 45 oriented wafer orientation was observed compared to standard wafer. Furthermore, wafering shows no impact of wafer orientation on wafer's topology (Table 6).

**Table 6:** Wafer topology, comparison between M2 45° oriented wafer and standard wafers. Values averaged over 60 wafers- CEA

	Standard M2 wafers ( $\mu$ m)	M2 45° oriented wafers ( $\mu$ m)
Average thickness	159.17	159.29
TTV	8.39	9.12
Bow	9.03	11.74

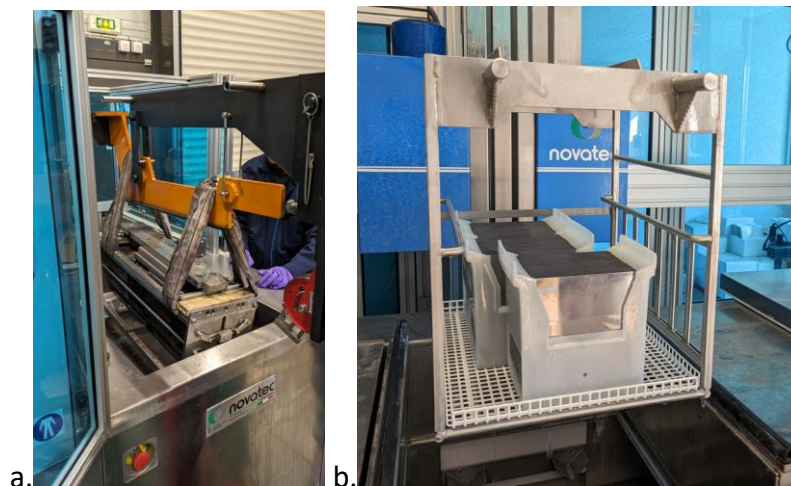


**Figure 14:** Norsun M2 „standard“ wafers a. wafer pre-cleaning; b. wafer cleaning – Novatec equipments

## 6 Conclusion

An innovative cut-cell cleavage process was elaborated and validated at CEA at laboratory scale. This process is based on 45° rotation during silicon brick and wafers fabrication, allowing the alignment of the preferential cleavage plane (110) with the solar cells bus bars. In this IBC4EU project, CEA collaborated with industrial partners to the adaptation and compliance of this 45° approach to larger ingot/brick sizes and alternative doping configurations. Finally, full evaluation of the wafer produced with industrial integration requirements needed to be assessed. Two series of 45° oriented squaring were thus performed according to partners's constraints regarding wafer size for further PV cell integration, allowing the manufacturing of the two following bricks: a p-type Cz ingot doped with boron from Kalyon in G1 size and a p-type Cz ingot doped with gallium from Norsun in M2 size. For both configurations the (110) plane misorientations obtained after grinding were less than 0.3° which allows a pure mechanical cleavage between the metallization busbars of the future PV cells. Wafer preparation steps also demonstrate full compliance of the 45° rotation with existing production tools, as no increase of breakage rate was observed when compared to standard wafers.

Finally, the G1 45° oriented p-type wafers produced were processed on Kalyon's PERC production line. Results obtained at both cell and module level are very promising, with similar final efficiencies and breakage rates achieved, demonstrating here again the very good compliance of the 45° rotated approach with full industrial environment requirements. With this deliverable, we thus show that the 45° rotated wafer based approach developed by CEA can be integrated in full production environment, can be compatible with large final wafer/brick size, and allows a significant simplification of the cell cut-step, opening new alternative technological solutions to the traditional laser-based processes usually considered.

## 7 Glossary

Cz	Czochralski
NS	Norsun
Ka	Kalyon
SHJ	Solar heterojunction cell
PV	Photovoltaic
VIVP	Vehicle integrated photovoltaics
BIPV	Building integrated photovoltaics
PERC	Passivated Emitter and Rear Ce

## 8 References

1. J.F. Lelievre *et al.*, Alternative Cz Ingot Squaring And Half Cells Cutting Methodology for Low Temperature PV Cell and Module Technologies, Presented at the 37th European PV Solar Energy Conference and Exhibition, EU-PVSEC), 2020.
2. S. Harrison *et al.* EU PVSEC 2021 proceedings: 38th. 2021. doi: 10.4229/EUPVSEC20212021-2BO.15.3
3. S. Harrison *et al.* , simplified cell cutting, efficient edge passivation, copper metallization: tackling the last hurdles for optimized shj integration in shingle module configuration, 8th World Conference on Photovoltaic Energy Conversion, 2023
4. ITRPV 2018, "International technology roadmap for photovoltaic (ITRPV): 2017 results", 9th edn (Mar.)
5. S.Harrison *et al.*, "Silicon Heterojunction and Half-cell configuration: optimization path for increased module power", Proc.of the 46th IEEE PVSC, Chicago, 2019.
6. A.Fell *et al.*, "Modeling edge recombination in silicon solar cells", IEEE J.Photovolt, Vol8, No2, pp428-434, 2018
7. M.Albaric *et al.* , "Alternative Cz Ingot squaring and cell cutting methodology for low temperature Silicon-based PV cells" CSSC-11 2022
8. M.Albaric *et al.* , "Process optimizations for edge passivation and high efficiency shingle heterojunction cells compatible with industry" , EU PVSEC 2023